ChemComm
Chemical Communications

Accepted Manuscript

This article can be cited before page numbers have been issued, to do this please use: N. Boysen, B. Misimi, A. Muriqi, J. Wree, T. Hasselmann, D. Rogalla, T. Haeger, D. Theirich, M. Nolan, T. Riedl and A. Devi, *Chem. Commun.*, 2020, DOI: 10.1039/D0CC05781A.

ROYAL SOCIETY OF CHEMISTRY

rsc.li/chemcomm

View Article Online
DOI: 10.1039/D0CC05781A

COMMUNICATION

A carbene stabilized precursor for the spatial atomic layer deposition of copper thin films

Received 00th January 20xx,
Accepted 00th January 20xx

DOI: 10.1039/x0xx00000x

Nils Boysen,[a] Bujamin Misimi,[b] Arbresha Muriqi,[c] Jan-Lucas Wree,[a] Tim Hasselmann,[b] Detlef Rogalla,[d] Tobias Haeger,[b] Detlef Theirich,[b] Michael Nolan,[e] Thomas Riedl,[b*] and Anjana Devi [a*]

This paper demonstrates a carbene stabilized precursor [Cu(^{tBu}NHC)(hmds)] with suitable volatility, reactivity and thermal stability, that enables the spatial plasma-enhanced atomic layer deposition (APP-ALD) of copper thin films at atmospheric pressure. The resulting conductive and pure copper layers were thoroughly analysed and a comparison of precursor and process with the previously reported silver analogue [Ag(^{tBu}NHC)(hmds)] revealed interesting similarities and notable differences in precursor chemistry and growth characteristics. This first report of APP-ALD grown copper layers is an important starting point for high throughput, low-cost manufacturing of copper films for nano- and optoelectronic devices.

Copper possesses a very low electrical bulk resistivity ρ = 0.168 μΩ cm at room temperature which is comparable to that of silver.[1] The high melting point of Cu, low temperature coefficient of resistivity, reduced tendency for electromigration compared to Al or Ag,[2–4] and lower cost than Au or Ag render Cu a favourable choice as electrode material for a variety of applications, such as microelectronics, photovoltaics and thin film (opto-)electronics.[5–8] Atomic layer deposition (ALD) affords thin films with excellent homogeneity, conformality and precise thickness control even on high-aspect ratio structures as required for the aforementioned applications.[9] On the other hand, ALD processes typically require long processing times due to time sequenced surface reactions with the precursors and the use of expensive vacuum equipment with overall low throughput.[10] These limitations can be overcome by the use of spatial ALD (SALD), that translates the time sequenced precursor delivery into a spatially separated one with a moving substrate.[11,12] It has been shown that SALD can even be performed at atmospheric pressure without the need for expensive vacuum equipment.[13–15] In general, the use of plasma as co-reactant in an ALD process can reduce the deposition temperature drastically and is therefore preferable for the deposition on temperature sensitive substrates.[16] Some ALD processes exclusively function with a plasma-activated species as co-reactant.[17] The spatial plasma enhanced atomic layer deposition at atmospheric pressure (APP-ALD) is therefore an important development to widen the scope for low-cost, high throughput ALD manufacturing. While APP-ALD has been demonstrated for a number of metal-oxides,[18,19] the growth of metals by APP-ALD is still in its infancy.[20–22] Further progress in the field critically relies on the development of metal precursors that are volatile, thermally stable and reactive,[23–25] while also other factors, such as adhesion layers,[26] different reducing agents,[27–29] or low deposition temperature must also be taken into account.[30] For the ALD of Cu metal, plasma activated processes with different classes of precursors are known (Supporting Information (SI), Table S1).[30–35] A recent systematic study by Coyle et al. featured different heteroleptic, monomeric Cu(I) complexes stabilized by N-heterocyclic carbenes (NHCs) and a reactive bis(trimethylsilyl)amide (hmds) N-coordinating anionic ligand.[36] Proof-of-principle depositions were carried out at a high temperature of 225 °C with [Cu(^{iPr}NHC)(hmds)] and resulted in thin Cu nanostructures on Si substrates with growth rates of 0.2 Å/cycle.[35] Although a variety of precursors has been implemented for the plasma-assisted ALD of Cu, many of them do not qualify for APP-ALD. In fact, no APP-ALD of Cu thin films has been reported so far. We have previously shown that [Ag(^{tBu}NHC)(hmds)] provided excellent results in the APP-ALD of thin Ag thin films.[20] An analogous Cu compound, (1,3-di-*tert*-butyl-imidazolin-2-ylidene) copper(I) bis(trimethylsilyl)amide [Cu(^{tBu}NHC)(hmds)] was described to provide outstanding thermal stability and volatility.[36] However, no reports about the use of this compound for ALD exist. Furthermore, structural characteristics of the compound, such as crystallographic data, that might explain the properties of the compound are

[a] *Inorganic Materials Chemistry, Ruhr University Bochum, 44801 Bochum, Germany*
[b] *Institute of Electronic Devices and Wuppertal Center for Smart Materials & Systems, University of Wuppertal, 42119 Wuppertal, Germany*
[c] *Tyndall National Institute, University College Cork, Lee Maltings, Dyke Parade, Cork T12 R5CP, Ireland*
[d] *RUBION, Ruhr University Bochum, 44801 Bochum, Germany*
[e] *Tyndall National Institute, University College Cork, Lee Maltings, Dyke Parade, Cork T12 R5CP, Ireland and Nanotechnology and Integrated Bioengineering Centre, Ulster University, Shore Road, Co Antrim, BT37 OQB, Northern Ireland*
Electronic Supplementary Information (ESI) available. See DOI: 10.1039/x0xx00000x

unknown. To exploit the potentially beneficial properties of this precursor for APP-ALD, we first optimized the synthetic strategy, extended the missing analytical data by single crystal X-ray diffraction (SC-XRD) and compared the evaporation behaviour to that of the analogous silver precursor [Ag($^{t\text{Bu}}$NHC)(hmds)], reported by us for APP-ALD of Ag.[20] The geometry of the two complexes were compared employing density functional theory (DFT) studies which revealed significant differences in the bond dissociation energies that could be correlated to the dissimilarity in the stability and reactivity of the two compounds. Finally, we employed [Cu($^{t\text{Bu}}$NHC)(hmds)] in APP-ALD as a first demonstration of the deposition of conductive Cu metal thin films at atmospheric pressure and low temperatures. These results pave the way towards low-cost and high-throughput APP-ALD of Cu thin films for a wide range of large-area applications.

The target precursor was synthesized by modifying the procedure reported earlier.[36] A substantial improvement was achieved in terms of reducing the reaction steps necessary to obtain the product and scalability of the synthesis (Scheme 1). It should be noted that the one-pot synthetic strategy is advantageous as it is conveniently realized for larger reaction scales, which were tested up to isolated product sizes of 12 g in this study. The new route employed enables a straightforward scale-up of the precursor particularly needed for high-throughput ALD. The spectroscopic purity and structural integrity of the compound was confirmed by ^{1}H- and ^{13}C-NMR spectroscopy and are in accordance with the already reported values (see SI, Figure S1-S2).[36] The most interesting signal at 201.6 ppm in the ^{13}C-NMR spectrum can be attributed to the carbenic carbon, which is shifted downfield when compared to its directly related congener [Ag($^{t\text{Bu}}$NHC)(hmds)] (205.1 ppm) and is explained by a higher extent of π-electron backdonation.[20,37] This indicates the formation of a strong Cu–C bond which is in accordance with the findings by SC-XRD (Figure 1, Table S2-S8). The complex crystallizes in a triclinic system with a close packing in the space group $P\bar{1}$, while the monomeric state in the solid state is retained and no Cu–Cu interactions are visible between the discrete molecules within the crystal packing. A linear coordination of the NHC and amide (hmds) ligand around the Cu nucleus is highlighted by a C–Cu–N angle of 178.1° as typically seen for monomeric linear NHC Cu(I) complexes.[38]

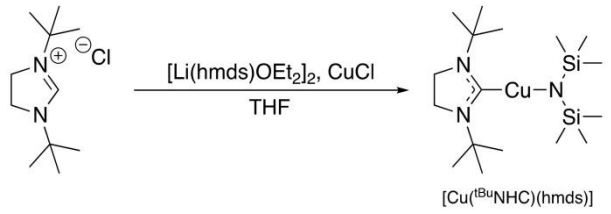

Scheme 1. Reaction pathway for the one-pot synthesis of [Cu($^{t\text{Bu}}$NHC)(hmds)].

The bond length of the Cu–C bond (1.901 Å) is in the range of other copper NHC complexes,[39] while the Cu–N bond (1.865 Å) is significantly shorter than in the [Cu(hmds)]$_4$ tetramer (1.919 Å).[40] Compared to the directly related Ag complex [Ag($^{t\text{Bu}}$NHC)(hmds)], the molecular structure is nearly identical, but due to the significantly larger mono-cationic radius of Ag (1.89 Å vs. 1.73 Å),[41] the bond lengths of Ag–N (2.079 Å) and Ag–C (2.095 Å) are larger than for Cu–N and Cu–C in the solid crystalline state.

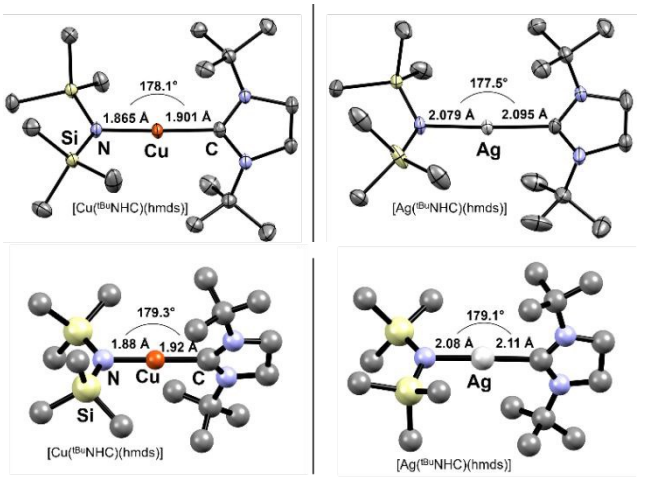

Figure 1. Top: Molecular crystal structures of [Cu($^{t\text{Bu}}$NHC)(hmds)] and [Ag($^{t\text{butyl}}$NHC)(hmds)] (from CCDC ref. NIMMEE) (left).[20] Hydrogen atoms and disorders are omitted for clarity, while the thermal ellipsoids are drawn with 50% probability. Bottom: DFT relaxed atomic structures of [Cu($^{t\text{Bu}}$NHC)(hmds)] and [Ag($^{t\text{Bu}}$NHC)(right)].

Additionally, the geometries of the complexes were determined by DFT calculations (Figure 1, bottom) which show that [Cu($^{t\text{Bu}}$NHC)(hmds)] consists of shorter M–C and M–N bond lengths (1.92 Å and 1.88 Å) compared to [Ag($^{t\text{Bu}}$NHC)(hmds)] (2.11 Å and 2.08 Å). The bonding angles around M at N-M-C are 179.3° for [Cu($^{t\text{Bu}}$NHC)(hmds)] and 179.1° for [Ag($^{t\text{Bu}}$NHC)(hmds)]. The bond dissociation energy defined as the energy for the removal of the hmds ligand was computed for Ag($^{t\text{Bu}}$NHC)(hmds) and Cu($^{t\text{Bu}}$NHC)(hmds). It is found that for the Ag($^{t\text{Bu}}$NHC)(hmds) precursor, the bond dissociation energy is 341.31 kJ/mol while for Cu($^{t\text{Bu}}$NHC)(hmds) this energy is 446.33 kJ/mol. The lower bond dissociation energy confirms the higher reactivity of the Ag–N bond in Ag($^{t\text{Bu}}$NHC)(hmds) compared to Cu($^{t\text{Bu}}$NHC)(hmds). These XRD and DFT results indicate the presence of stronger Cu–C/Cu–N interactions in [Cu($^{t\text{Bu}}$NHC)(hmds)] which are effectively shielding the highly reactive Cu nucleus leading to a monomeric compound as desired for its application in ALD. To investigate the thermal stability and evaporation behaviour, thermogravimetric analysis (TGA) was carried out with [Cu($^{t\text{Bu}}$NHC)(hmds)] and the results were compared to [Ag($^{t\text{Bu}}$NHC)(hmds)]. The compound features a single step evaporation behaviour with an onset of evaporation at 110 °C and a residual mass of 2.4 % (Figure 2). Interestingly, the parent silver precursor features a very similar onset of evaporation at 133 °C, but a significantly higher residual mass of 20.2 %, which could be attributed to a substantial thermal decomposition at higher temperatures. These similarities in the evaporation behaviour at low temperatures and differences in thermal stability at higher temperatures could be explained by the intrinsic molecular structure of the complexes. The larger and thus weaker C–Ag–

N bonds in [Ag(^{tBu}NHC)(hmds)] might generally explain its lower thermal stability compared to [Cu(^{tBu}NHC)(hmds)], but the nearly identical molecular structure explain the close onset of evaporation points due to similar intermolecular van-der-Waals interactions. Again, we used DFT calculations to further understand the precursor chemistry at molecular level and get an insight into the reactivity and stability of the precursors. To assess their reactivity, we have built models of [Cu(^{tBu}NHC)(hmds)] and [Ag(^{tBu}NHC)(hmds)] precursors in presence of hydrogen. The H_2 molecule was placed at a distance of 1.70 Å from the metals. Figure S4a shows that for [Cu(^{tBu}NHC)(hmds)] the H_2 molecule does not react with the precursor.

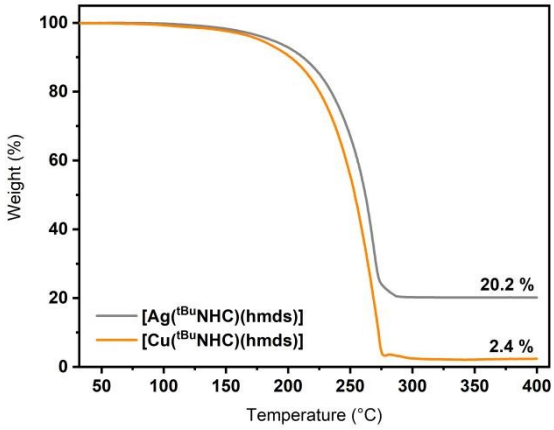

Figure 2. Thermogravimetric analysis curves of [Cu(^{tBu}NHC)(hmds)] (red) and [Ag(^{tBu}NHC)(hmds)] (grey) for comparison.

In contrast to Cu, the Ag precursor reacts with H_2 breaking the Ag-N bond and forming a new Ag-H bond with distance 1.16 Å and a new N-H bond with distance 1.03 Å (Figure S4b). The computed interaction energy upon forming the Ag-H and N-H bonds is –0.27 eV. This set of calculations confirms the higher reactivity of Ag precursor compared to Cu precursor towards H_2. The promising thermal properties of [Cu(^{tBu}NHC)(hmds)] and its intrinsic reactivity upon exposure to air (see SI, Figure S3 and S5) manifest this precursor as an exceptionally promising candidate for the APP-ALD of Cu metal films. Thus, [Cu(^{tBu}NHC)(hmds)] was applied as a precursor in an APP-ALD process for the deposition of copper metal layers. A home-built APP-ALD system with a plasma source based on a dielectric barrier discharge (DBD) was used, as described in more detail in our earlier work.[42] The substrate and precursor temperature was kept at 100 °C for all Cu experiments and borosilicate glass or silicon were used as substrate materials. Figure 3a shows the Cu atom coverage (atoms/area) as determined by Rutherford backscattering spectrometry (RBS) vs. number of ALD cycles. A growth rate (GR) of 2.0 x 10^{14} Cu atoms/(cm^2 cycle) could be derived, which corresponds to an equivalent of 0.23 Å/cycle considering the bulk density of Cu. For comparison, we included atom coverage for an APP-ALD process of Ag grown with the analogous precursor [Ag(^{tBu}NHC)(hmds)]. The resulting GR of 4.5 × 10^{14} Ag atoms/(cm^2 cycle), equivalent to 0.76 Å/cycle, is more than twice that of the Cu process. The lower GR of the [Cu(^{tBu}NHC)(hmds)] precursor may be related to different reactivity on the substrate surface because of the shorter and thus stronger N–Cu–C bonds, as discussed above. To verify the expected saturation behaviour in our ALD process, we successively increased the amount of precursor delivered to the substrate surface, by varying the N_2 flow through the Cu bubbler in a range from 0.25 slm up to 4 slm (Figure 3b). Note, our setup did not allow us to further reduce the flow through the Cu bubbler below 0.25 slm. In this range we identified a constant average mass coverage of (1.7 ± 0.2) × 10^{17} Cu atoms/cm^2 and a constant area coverage of 60 ± 2 %. We envisage that the higher stability of the Cu precursor compared to the analogous Ag precursor might require a further increased delivery of hydrogen plasma to reach a similar GR as that found in the case of Ag. Due to technical limitations, the APP-ALD setup used already operates at the maximum of hydrogen plasma delivery.

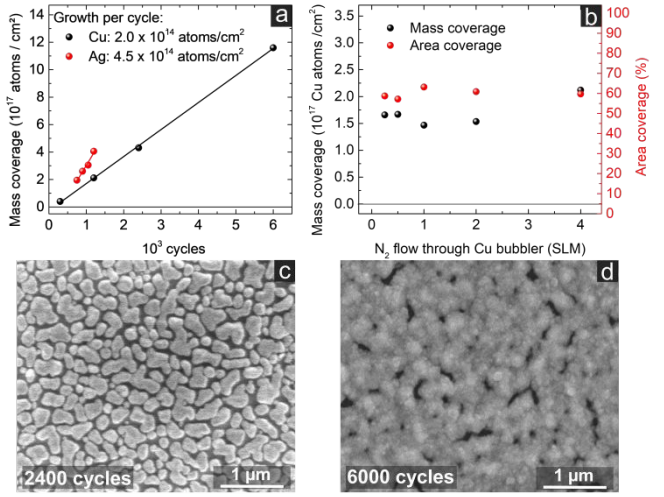

Figure 3. a) Atom coverage as determined by RBS vs. number of ALD cycles for Cu and Ag. b) Atom and area coverage vs. Cu precursor dosing for 1200 growth cycles. c) SEM images of Cu layers grown by APP-ALD at 100 °C using 2400 cycles and d) 6000 cycles.

Figure 3c shows an SEM image of a Cu layer grown with 2400 cycles (Cu atom coverage of about 4.3 × 10^{17} atoms/cm^2). As expected for the growth of a metal layer on a substrate with lower surface energy, the Cu forms islands that are not percolated, and the layer does not show lateral conductivity. The onset of percolation is found at about 10^{18} atoms/cm^2. At 6000 cycles, R_{sh} is 2.1 Ω/sq ($\rho = 2.9 \times 10^{-5}$ Ω cm) and the corresponding SEM image displays an almost entirely percolated Cu film (Figure 3d). The deposited Cu layer at 6000 cycles shows a surface roughness of R_q = 13.2 nm (Figure S6). These results represent the first example of percolated and conductive Cu layers grown by APP-ALD. Also striking is that X-ray photoelectron spectroscopy (XPS) revealed that all potential contaminants related to the Cu-precursor, i.e. Si, N or C, were below the detection limit of the measurement (< 0.5 at. %) (Figure S7). The core level spectrum of Cu2p indicates the predominant presence of Cu(0) with only some trace amounts of oxidized Cu (e.g. CuO) (Figure S8).[43–45] This investigative study is a significant contribution to the field of metal ALD where for the first time conductive copper deposition by APP-ALD could be realised using a reactive carbene based precursor.

Conclusions

In summary, we report the carbene stabilized [Cu(^{tBu}NHC)(hmds)] as an excellent precursor for the APP-ALD of Cu thin films. The precursor meets the demanding characteristics for ALD in terms of high volatility, thermal stability, and reactivity, while its synthesis is easily scalable. It features a comparable volatility but substantially higher thermal stability when compared to the already reported and directly related APP-ALD precursor [Ag(^{tBu}NHC)(hmds)], which is correlated to the intrinsic differences in reactivity of both precursors as shown by DFT calculations. Subsequently, [Cu(^{tBu}NHC)(hmds)] was employed for APP-ALD growth studies at 100 °C resulting in highly conductive and percolated (resistivity $2.9 \times 10^{-5}\,\Omega\,\mathrm{cm}$) Cu thin films with a GR of 0.23 Å/cycle and high purity. The higher GR of 0.76 Å/cycle with the corresponding APP-ALD process using [Ag(^{tBu}NHC)(hmds)] directly correlates with differences seen in the intrinsic precursor chemistry of both compounds. This first APP-ALD process for Cu metal not only enables thin films of Cu to be applied in a high throughput and low-cost environment, but also its sets up new avenues for further developments in the field of precursor tuning as well as nanoscale processing of metal films at atmospheric pressure. The obtained Cu films have serious potential for applications as electrodes which is the subject of our forthcoming work.

Conflicts of interest

There are no conflicts of interests to declare.

Acknowledgement

The work was funded by the Deutsche Forschungsgemeinschaft (DFG) under the project numbers DFG-DE 790-18-1 and RI1551/13-1. We also acknowledge the support from the European Commission through the H2020 MSCA Network HYCOAT, Grant 765378, and access to the Science Foundation Ireland supported computing resources at Tyndall.

Notes and references

1 R. A. Matula, *J. Phys. Chem. Ref. Data.*, 1979, **8**, 1147–1298.
2 J. A. Cahill and A. D. Kirshenbaum, *J. Phys. Chem.*, 1962, **66**, 1080–1082.
3 J. H. Dellinger, *The Temperature Coefficient of Resistance of Copper*, U.S. Government Printing Office, 1911.
4 T. Nitta, *J. Electrochem. Soc.*, 1993, **140**, 1131.
5 B. Li, T. D. Sullivan, T. C. Lee and D. Badami, *Microelectron. Reliab.*, 2004, **44**, 365–380.
6 P. Bellchambers, M. Walker, S. Huband, A. Dirvanauskas and R. A. Hatton, *ChemNanoMat*, 2019, **5**, 619–624.
7 M. Stoppa and A. Chiolerio, *Sensors*, 2014, **14**, 11957–11992.
8 J. Zhao, X. Zheng, Y. Deng, T. Li, Y. Shao, A. Gruverman, J. Shield and J. Huang, *Energy Environ. Sci.*, 2016, **9**, 3650–3656.
9 S. M. George, *Chem. Rev.*, 2010, **110**, 111–131.
10 R. W. Johnson, A. Hultqvist and S. F. Bent, *Materials Today*, 2014, **17**, 236–246.
11 D. Muñoz-Rojas and J. MacManus-Driscoll, *Mater. Horiz.*, 2014, **1**, 314–320.
12 P. Poodt, D. C. Cameron, E. Dickey, S. M. George, V. Kuznetsov, G. N. Parsons, F. Roozeboom, G. Sundaram and A. Vermeer, *JVST A*, 2012, **30**, 010802.
13 Y. Creyghton, A. Illiberi, A. Mione, W. van Boekel, N. Debernardi, M. Seitz, F. van den Bruele, P. Poodt and F. Roozeboom, *ECS Trans.*, 2016, **75**, 11–19.
14 D. Muñoz-Rojas, V. H. Nguyen, C. Masse de la Huerta, S. Aghazadehchors, C. Jiménez and D. Bellet, *Comptes Rendus Physique*, 2017, **18**, 391–400.
15 D. H. Levy, D. Freeman, S. F. Nelson, P. J. Cowdery-Corvan and L. M. Irving, *Appl. Phys. Lett.*, 2008, **92**, 192101.
16 S. E. Potts, W. Keuning, E. Langereis, G. Dingemans, M. C. M. van de Sanden and W. M. M. Kessels, *J. Electrochem. Soc.*, 2010, **157**, P66.
17 H. C. M. Knoops, T. Faraz, K. Arts and W. M. M. (Erwin) Kessels, *J. Vac. Sci. Technol. A*, 2019, **37**, 030902.
18 L. Hoffmann, D. Theirich, S. Pack, F. Kocak, D. Schlamm, T. Hasselmann, H. Fahl, A. Räupke, H. Gargouri and T. Riedl, *ACS Appl. Mater. Interfaces*, 2017, **9**, 4171–4176.
19 L. Hoffmann, D. Theirich, D. Schlamm, T. Hasselmann, S. Pack, K. O. Brinkmann, D. Rogalla, S. Peters, A. Räupke, H. Gargouri and T. Riedl, *J. Vac. Sci. Technol. A*, 2018, **36**, 01A112.
20 N. Boysen, T. Hasselmann, S. Karle, D. Rogalla, D. Theirich, M. Winter, T. Riedl and A. Devi, *Angew. Chem. Int. Ed.*, 2018, **57**, 16224–16227.
21 A. Mameli, F. van den Bruele, C. K. Ande, M. A. Verheijen, W. M. M. Kessels and F. Roozeboom, *ECS Trans.*, 2016, **75**, 129–142.
22 F. J. van den Bruele, M. Smets, A. Illiberi, Y. Creyghton, P. Buskens, F. Roozeboom and P. Poodt, *JVST A*, 2015, **33**, 01A131.
23 T. J. Knisley, L. C. Kalutarage and C. H. Winter, *Coordination Chemistry Reviews*, 2013, **257**, 3222–3231.
24 M. Leskelä and M. Ritala, *Thin Solid Films*, 2002, **409**, 138–146.
25 A. Devi, *Coord. Chem. Rev.*, 2013, **257**, 3332–3384.
26 Z. Li, R. G. Gordon, D. B. Farmer, Y. Lin and J. Vlassak, *Electrochem. Solid-State Lett.*, 2005, **8**, G182.
27 K. Väyrynen, K. Mizohata, J. Räisänen, D. Peeters, A. Devi, M. Ritala and M. Leskelä, *Chem. Mater.*, 2017, **29**, 6502–6510.
28 T. J. Knisley, T. C. Ariyasena, T. Sajavaara, M. J. Saly and C. H. Winter, *Chem. Mater.*, 2011, **23**, 4417–4419.
29 L. C. Kalutarage, S. B. Clendenning and C. H. Winter, *Chem. Mater.*, 2014, **26**, 3731–3738.
30 Z. Guo, H. Li, Q. Chen, L. Sang, L. Yang, Z. Liu and X. Wang, *Chem. Mater.*, 2015, **27**, 5988–5996.
31 A. Niskanen, A. Rahtu, T. Sajavaara, K. Arstila, M. Ritala and M. Leskelä, *J. Electrochem. Soc.*, 2005, **152**, G25.
32 L. Wu and E. Eisenbraun, *J. Vac. Sci. Technol. B*, 2007, **25**, 2581.
33 C. Jezewski, W. A. Lanford, C. J. Wiegand, J. P. Singh, P.-I. Wang, J. J. Senkevich and T.-M. Lu, *J. Electrochem. Soc.*, 2005, **152**, C60.
34 D.-Y. Moon, D.-S. Han, S.-Y. Shin, J.-W. Park, B. M. Kim and J. H. Kim, *Thin Solid Films*, 2011, **519**, 3636–3640.
35 J. P. Coyle, G. Dey, E. R. Sirianni, M. L. Kemell, G. P. A. Yap, M. Ritala, M. Leskelä, S. D. Elliott and S. T. Barry, *Chem. Mater.*, 2013, **25**, 1132–1138.
36 J. P. Coyle, E. R. Sirianni, I. Korobkov, G. P. A. Yap, G. Dey and S. T. Barry, *Organometallics*, 2017, **36**, 2800–2810.
37 D. Tapu, D. A. Dixon and C. Roe, *Chem. Rev.*, 2009, **109**, 3385–3407.
38 A. J. Arduengo, H. V. R. Dias, J. C. Calabrese and F. Davidson, *Organometallics*, 1993, **12**, 3405–3409.
39 F. Lazreg and C. S. J. Cazin, in *N-Heterocyclic Carbenes*, ed. S. P. Nolan, Wiley-VCH Verlag GmbH & Co. KGaA, Weinheim, Germany, 2014, pp. 199–242.
40 P. Miele, J. D. Foulon, N. Hovnanian, J. Durand and L. Cot, *European Journal of Solid State and Inorganic Chemistry*, 1992, **29**, 573.
41 M. Rahm, R. Hoffmann and N. W. Ashcroft, *Chem. Eur. J.*, 2016, **22**, 14625–14632.
42 L. Hoffmann, D. Theirich, S. Pack, F. Kocak, D. Schlamm, T. Hasselmann, H. Fahl, A. Räupke, H. Gargouri and T. Riedl, *ACS Appl. Mater. Interfaces*, 2017, **9**, 4171–4176.
43 J. Haber, T. Machej, L. Ungier and J. Ziółkowski, *J. Solid State Chem.*, 1978, **25**, 207–218.
44 G. Schön, *Surface Science*, 1973, **35**, 96–108.
45 M. C. Biesinger, L. W. M. Lau, A. R. Gerson and R. St. C. Smart, *Appl. Surf. Sci.*, 2010, **257**, 887–898.

View Article Online
DOI: 10.1039/D0CC05781A